Collective Shift in Resonant Light Scattering by a One-Dimensional Atomic Chain

Antoine Glicenstein, Giovanni Ferioli, Nikola Šibalić, Ludovic Brossard, Igor Ferrier-Barbut,* and Antoine Browaeys
Université Paris-Saclay, Institut d'Optique Graduate School, CNRS, Laboratoire Charles Fabry, 91127 Palaiseau, France

(Received 11 April 2020; accepted 1 June 2020; published 25 June 2020)

We experimentally study resonant light scattering by a one-dimensional randomly filled chain of cold two-level atoms. By a local measurement of the light scattered along the chain, we observe constructive interferences in light-induced dipole-dipole interactions between the atoms. They lead to a shift of the collective resonance despite the average interatomic distance being larger than the wavelength of the light. This result demonstrates that strong collective effects can be enhanced by structuring the geometrical arrangement of the ensemble. We also explore the high intensity regime where atoms cannot be described classically. We compare our measurement to a mean-field, nonlinear coupled-dipole model accounting for the saturation of the response of a single atom.

DOI: 10.1103/PhysRevLett.124.253602

Two scatterers illuminated by a resonant light field are coupled to each other as the field radiated by one acts on the other, giving rise to a light-induced resonant dipole-dipole interaction. In a disordered ensemble containing many emitters, the random relative phases of the radiated fields lead to destructive interferences suppressing the effect of interactions. Structuring the sample could allow recovering constructive interferences, thus, enhancing dipole interactions and shaping its collective coupling to resonant light [1–5]. Cold atoms provide an interesting platform for studying collective light-matter interaction, exhibiting negligible inhomogeneous broadening. Experiments on disordered samples of cold atoms already led to the observation of collective effects in near-resonant light scattering [6–15]. Realizing ordered atomic arrays to enhance the collective coupling to light requires controlled positioning of the individual atoms with subwavelength precision. This sets stringent experimental requirements, but provides new pathways for engineering strong collective light-matter coupling. For example, the interactions can lead to enhanced reflectivity for a single atomic layer [2,3,16], an effect recently demonstrated using ultracold atoms in two-dimensional optical lattices [17]. In 1D arrays, it was predicted that interactions induce subradiant transport in atomically thin wires [18–22]. These predictions rely on models based on linear coupled dipoles (e.g., [23]), or small scale full quantum models [22,24,25]. This restricts the analysis either to the weak driving limit where a classical model is valid, or to small ensembles of up to about a dozen atoms, where full quantum calculations can be done. Experimentally, collective scattering with one-dimensional systems has been observed with atoms trapped near nanophotonic waveguides or nanofibers [26–30], and with chains of up to eight trapped ions [31].

In this Letter, we study resonant light scattering by a one-dimensional chain of two-level atoms as considered theoretically, e. g., in [21,32,33]. For this, we present a platform realizing a free-space, 1D partially filled chain of up to 100 atoms. We measure the intensity spectrum of the light scattered perpendicular to it. By local and global measurements of the resonance frequency shift, we show that collective constructive interferences in resonant dipole-dipole interactions lead to an enhancement of the shift with respect to random dense ensembles [7,11,14,15]. Finally, we extend our experiments beyond the weak driving limit and observe a suppression of the interaction-induced shift. We compare our findings to a model based on nonlinear coupled dipoles [34].

To illustrate how the dimensionality of the atomic ensemble enhances collective scattering, consider a 1D chain of atoms excited by a plane wave (frequency $\omega = kc$) propagating along the chain axis $\hat{z}$ (Fig. 1) as proposed in [32]. In the low-intensity limit, the dipoles respond linearly to the field E [35], i. e., the dipole of atom n at position z_n is $d_n = \varepsilon_0 \alpha E(z_n)$, with $\alpha = i(6\pi/k_0^3)/(1 - 2i\Delta/\Gamma_0)$ the atomic polarizability. Here, $k_0 = 2\pi/\lambda_0$ is the transition wave vector, $\Delta = \omega - \omega_0$ the detuning with respect to the single-atom resonance frequency ω_0, and Γ_0 the linewidth. By propagating along $\hat{z}$, the driving field accumulates a phase kz_n on atom n. The induced dipole d_n scatters a field phase shifted by $\phi = \mathrm{Arg}(\alpha)$ with respect to the driving plane wave [36–39]. This scattered field accumulates a phase $k|z - z_n|$ by propagating along z. Therefore, in the forward direction ($z > z_n$), the phase accumulated by the field scattered by one atom is $kz + \phi$, independent of the position of the atom. Now, considering all atoms, the fields scattered in the forward direction are all in phase at first order (single scattering) and, thus, interfere constructively, as represented in Fig. 1(a). This conclusion only relies on the 1D geometry and holds even in the presence of position disorder along the chain. On the contrary, if the atoms are not aligned along the $\hat{z}$ axis, the phases accumulated by the scattered fields do

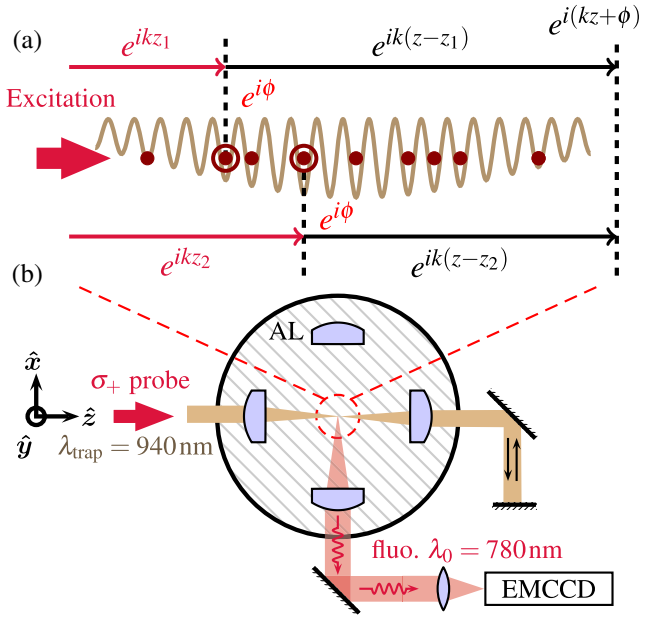

FIG. 1. (a) Chain of atoms under axial excitation. The total phase accumulated by propagation and single scattering is the same in the forward direction irrespective of the position of the atom. This results in constructive interferences of all forward scattered fields. (b) Schematic of the experimental setup. Two orthogonal high-resolution optical systems based on 4 in-vacuum aspheric lenses (AL) realize a chain of single atoms in a 1D-optical lattice and collect the scattered light on an EMCCD.

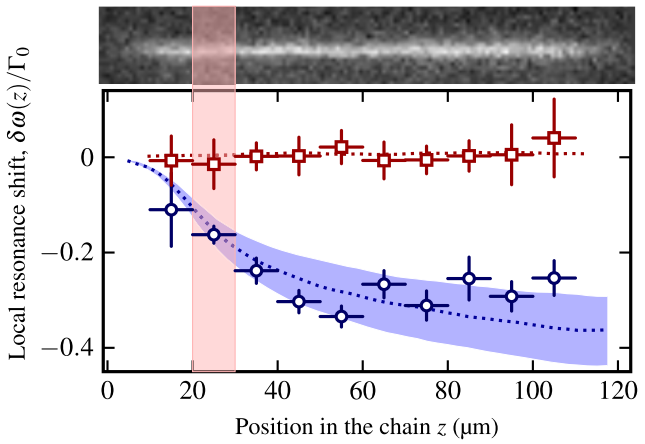

FIG. 2. Local shift $\delta\omega(z)$ as a function of the position in the chain. Blue circles (red squares): axial (transverse) excitation. Each data point is the resonance frequency of a 10 μm segment around z. Horizontal error bars: segment width. Vertical error bars: standard error of the fit of the local spectrum. Dotted lines: results of coupled-dipole simulations, with the shaded region corresponding to the experimental uncertainty in chain filling $\eta = 0.5 \pm 0.1$.

depend on their position, and their superposition in the forward direction does not lead to constructive interference.

To realize a 1D atomic chain and observe this effect, we introduce a new platform. We produce an optical lattice by retroreflecting a tight optical tweezer focused by two in-vacuum aspheric lenses with numerical aperture NA = 0.5 [Fig. 1(a)]. It yields a chain of traps with small intertrap spacing (trapping wavelength $\lambda_{\mathrm{trap}} = 940$ nm resulting in 470 nm spacing), similar to [40], but with tight transverse confinement. The trap beam waist $w_{\mathrm{trap}} = 3.3$ μm (Rayleigh range $z_R \simeq 36$ μm) is chosen to avoid strong variations of the radial confinement along the chain while keeping small trap volume [41]. The dipole trap depth at the waist is ∼3 mK, corresponding to peak transverse and longitudinal oscillation frequencies of, respectively, $\omega_\rho = 2\pi \times 50$ kHz and $\omega_z = 2\pi \times 750$ kHz. Another asset of our setup is the introduction of a second pair of aspheric lenses on a transverse axis as used in [42] for trapping and probing single atoms, here, allowing for local measurements along the lattice axis. The resolution of this system is ∼1 μm.

We load the lattice with ^{87}Rb atoms using the following sequence: We start from a 3D magneto-optical trap (MOT) superimposed to the lattice and, then, apply a 200 ms Λ-enhanced grey molasses on the D_1 line [43–45] with the lattice tweezer on. We found, empirically, that applying the molasses results in a more reliable loading of the chain with respect to direct MOT loading. Thanks to the low photon scattering rate of grey molasses, the lattice is filled with an average of more than one atom per site. Then, we switch the MOT beams back on for 5 ms. This pulse induces strong light-assisted collisions and ejects atoms out of shallow traps. The atoms are then optically pumped in the $|5^2S_{1/2}, F = 2, m_F = 2\rangle$ state, with the quantization axis set by a 0.5 G magnetic field aligned with the chain. At the end of the loading sequence, the 200 central lattice sites are loaded with an average filling $\eta = 0.5 \pm 0.1$. Thus, the average interatomic distance is $\langle r_{\mathrm{nn}} \rangle \simeq \lambda_{\mathrm{trap}} \simeq 1.2\lambda_0$ (here, $\lambda_0 \simeq 780$ nm). The average loading is measured by illuminating the chain with a saturating resonant beam in free flight and comparing the fluorescence of the whole chain (see example of an average image in Fig. 2) with that of a single atom calibrated independently. The final temperature is $T = 80(20)$ μK, yielding a transverse width $\sigma_\rho \simeq 300$ nm $\simeq 0.38\lambda_0$.

Using this platform, first, we explore collective scattering in the low-intensity limit. The atoms are excited along the chain axis by applying 200-ns pulses of a σ_+-polarized probe at $\lambda_0 = 780.2$nm (D_2 line). The probe waist is $w_{\mathrm{probe}} = 20$ μm (Rayleigh range $z_R = 1.6$ mm) such that it approximates a plane wave. The probe intensity is $I/I_{\mathrm{sat}} \simeq 0.3$. We image the light scattered by the atoms in the transverse direction on an electron multiplying CCD camera (EMCCD), through one of the two additional high-NA lenses. For a given probe detuning, the chain is illuminated by 50 probe pulses, and we repeat over 300 identically prepared samples to obtain sufficient statistics. The scattered intensity spectrum is extracted by repeating this at different detunings between $\Delta = -3\Gamma_0$ and $3\Gamma_0$. To reveal the effect of interactions along the chain, we

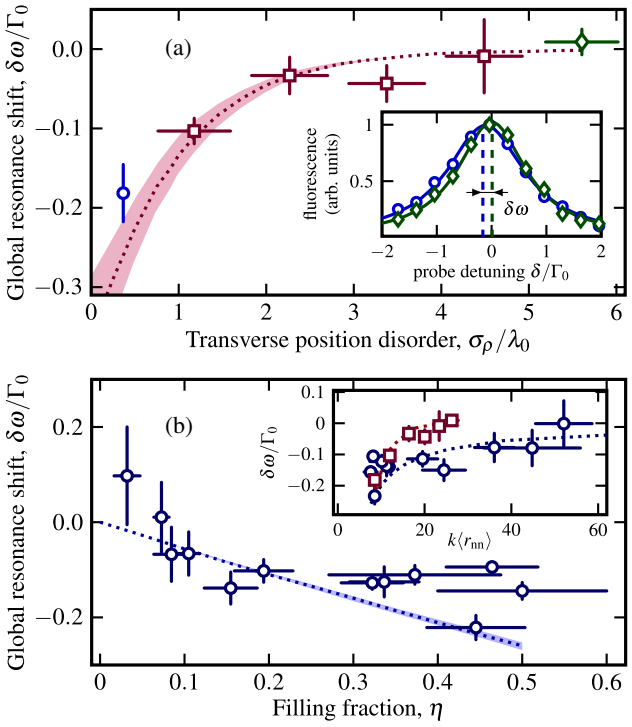

FIG. 3. (a) Global shift $\delta\omega$ as a function of the radial size σ_ρ of the cloud after a time of flight. Vertical error bars: fit standard errors, horizontal errors: size variation during probe pulse. Dotted line: coupled dipole simulations accounting for the experimental uncertainty on the chain filling η. Inset: example of fluorescence spectra. (b) Global shift $\delta\omega$ vs η compared to coupled dipole simulations (shaded region accounting for experimental uncertainty in temperature 80(20) μK. Vertical error bars: fit standard errors. Horizontal errors: experimental uncertainties. The reference of the shifts is the intercept of a linear fit of the data. Inset: comparing data of (a) and (b), plotted vs nearest-neighbor distance: $k\langle r_{nn}\rangle$.

divide it into 10 μm-long segments, as shown on the top of Fig. 2. We observe resonance profiles that are well fitted by a Lorentzian line shape, from which we extract the local shift of the resonance $\delta\omega(z)$ [inset, Fig. 3(a)]. This on-axis excitation is compared to the result of an identical excitation procedure but with a plane wave probe ($w_{\text{probe}\perp} \simeq 1.5$ mm) sent perpendicularly to the chain. The results are plotted in Fig. 2. Under perpendicular excitation, we do not observe any shift along the chain, while the shift does increase along the chain for the axial excitation, indicating a buildup of the interactions. These findings are in agreement with the qualitative discussion above. For comparison, shifts of comparable amplitude were obtained in disordered 2D and 3D samples but for interatomic distances about ten times smaller [7,14], highlighting the enhancement of the collective response by reducing the dimensionality.

Now, we describe our experimental results in terms of the steady-state coupled-dipole model [46]. In this model, each atomic dipole of the chain is driven by the field of the plane wave and the sum of the fields radiated by all the other atoms: $d_n = \epsilon_0\alpha[E_L(\boldsymbol{r}_n) + \sum_{m\neq n} G(\boldsymbol{r}_n - \boldsymbol{r}_m)d_m]$ with $G(\boldsymbol{r})$ the Green's function [47]. Here, we assume scalar dipoles to reproduce the experimental arrangement of two-level atoms driven by a σ_+-polarized field [50]. To get an intuitive understanding of the shift increase along the chain, first, we use a perturbative approach, as done in [32]. In the limit of large interparticle distance ($k_0\langle r_{nn}\rangle > 1$), only the long-range part of the radiated field plays a role and $G(\boldsymbol{r}) \propto e^{ikr}/kr$. Keeping only forward scattering at first order (single scattering), the field intensity at position z_n is [32,47]

$$|E^{(1)}(z_n,\Delta)|^2 = |E_L|^2\left(1 - \frac{6\Delta/\Gamma_0}{1+(2\Delta/\Gamma_0)^2}\sum_{z_m<z_n}\frac{1}{k|z_m - z_n|}\right), \tag{1}$$

with E_L the laser field amplitude. This simple model shows that the field seen by atoms down the chain is increased for red detunings ($\Delta < 0$). Thus, the excitation probability $|d_n^{(1)}(\Delta)|^2 \propto |E^{(1)}(z_n,\Delta)|^2/[1+(2\Delta/\Gamma_0)^2]$ is redshifted compared to the single-atom resonance due to the interactions. This interaction-induced shift is actually the equivalent of a collective Lamb shift [51] for a discrete medium [17,31]. The interpretation is the following: for red detunings, the scattered and driving fields are in phase ($\phi < \pi/2$) such that constructive interferences increase the field intensity $|E(z_n)|^2$ [52]. For blue detuning, they are out of phase ($\phi > \pi/2$) and their destructive interferences reduce $|E(z_n)|^2$.

Though the simple perturbative model captures the mechanism behind the local shift, full solutions of the coupled dipoles including experimental imperfections are necessary for a quantitative comparison with the data. Thus, we numerically solve the set of linear coupled equations to calculate each dipole $d_n(\Delta)$ for various detunings. The power emitted by a dipole is proportional to $\text{Im}[d_n E(z_n)^*] \propto |d_n|^2$. We take into account both the random filling fraction and the residual thermal fluctuation of the atomic positions (radially and axially) in each well by averaging over several hundreds of random realizations, and we plot the mean dipole in the chain slices used in the experiment, $\sum_{n\in\text{slice}}|d_n(\Delta)|^2$, as a function of the detuning. The obtained spectra are well fitted by a Lorentzian line shape, from which we extract the theoretical line shift. The results are shown in Fig. 2, for different fillings η compatible with the experimental uncertainty. We obtain a good agreement between the data and the *ab initio* model with no adjustable parameter.

Next, we vary the parameters controlling the interaction strength. As discussed above, the collective enhancement of interactions relies on the 1D geometry. Therefore, first, we consider a situation away from 1D. In this case, if an atom is displaced by ρ_n perpendicularly to the chain axis, the phase factor on axis is $k|\boldsymbol{r} - \boldsymbol{r}_n| \simeq k|z - z_n| + k\rho_n^2/(2|z - z_n|)$.

Thus, the relevant factor for constructive interferences to occur at an axial distance Δz should be that the Fresnel number $\sigma_\rho^2/\lambda_0\Delta z \ll 1$, with σ_ρ the radial extent. This shows that when $\sigma_\rho/\lambda_0 \gg 1$, interferences should disappear. To check this experimentally, we change the radial size of the atomic distribution by letting the chain expand in free flight. After this time of flight, we send a near-resonant probe pulse for 10 μs along the chain and again collect the light scattered in the transverse direction. Now, we record the scattered intensity summed over all the chain for various detunings and extract the global shift of the resonance frequency $\delta\omega$. Figure 3(a) shows the evolution of $\delta\omega$ as a function of σ_ρ/λ_0. As expected, the shift, and hence, the interactions, vanishes when the atoms are not in a 1D geometry. The dotted lines correspond to coupled-dipole simulations computed with our experimental parameters. They are in good agreement with the data.

In another set of experiments, we increase the interatomic distance while keeping the 1D geometry by reducing the filling fraction of the chain [47]. The global shift as a function of the filling of the chain is shown in Fig. 3(b), together with the coupled-dipole simulations. We experimentally observe a reduction of the shift, as predicted. However, the calculated linear dependence is not clear in the data. This may be explained by a nonuniform filling along the chain. The same data are plotted in the insert as a function of the average interatomic nearest-neighbor distance $k\langle r_{\rm nn}\rangle$ and compared with the data of Fig. 3(a): at a given $k\langle r_{\rm nn}\rangle$, the shift is much stronger for a 1D sample. Again, this shows that collective scattering is enhanced in 1D.

Finally, we explore the evolution of the frequency shift when increasing the intensity of the driving field beyond the low-intensity limit. We, again, send the probe light along the chain axis and collect the transverse scattered light. We have verified that the higher intensity does not lead to significant extra atom losses and heating. We measure the scattered intensity spectrum integrated over the chain. When increasing the intensity of the probe light, we observe a broadening of the Lorentzian line, as well as a suppression of the global shift as shown in Fig. 4(a).

To model the data, we use a nonlinear coupled-dipole (NCD) model accounting for the nonlinear single atom response (see, also, [34]): We again solve the coupled-dipole equations, but now, using the nonlinear (NL) expression of the atomic polarizability for a strongly driven two-level atom given by the steady-state solution of the optical Bloch equations [53]: $\alpha_{\rm NL}(\Delta,\Omega) = i\{[(6\pi/k_0^3)(1+2i\Delta/\Gamma_0)]/[1+(2\Delta/\Gamma_0)^2+2\Omega^2/\Gamma_0^2]\}$. Here, $\Omega = dE/\hbar$ ($d^2 = 3\pi\varepsilon_0\hbar\Gamma_0/k_0^3$) is the Rabi frequency and E is the total field driving the atom, superposition of the laser field, and the one scattered by all other atoms. This model amounts to a mean-field theory where the many-body density matrix is factorized into a product of individual atomic density matrices [34,47,54,55]. To compare to the data, we calculate the fluorescence which is proportional to the sum of the excited state populations $\rho_{ee,n} = {\rm Im}[\rho_{eg,n}\Omega_n^*]/\Gamma_0$ of atoms in the chain (here $\rho_{eg,n} = d_n/2d$ is the atomic coherence between ground and excited states of atom n) [53]. By solving this model, we observe that the spectrum becomes slightly asymmetric. Nonetheless, to extract a shift, we fit the center of the spectrum ($-2 < \Delta/\Gamma_0 < 2$) with a Lorentzian, as done in the experiments. Considering first unity-filled short chains, we obtain a reduction of the global shift with increased driving strength [Fig. 4(b), solid lines]. To check the validity of this model, we compare it with the full solution that keeps quantum correlations into account [Fig. 4(b), circles] calculated as in Refs. [22,24] for a chain of six atoms: the NCD model satisfyingly captures the evolution of the shift for the considered interatomic spacing.

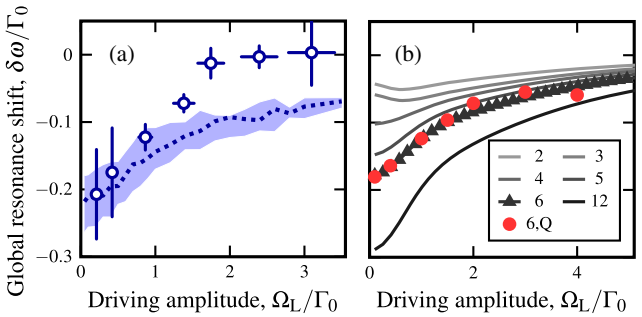

FIG. 4. (a) Measured global resonance shift as a function of the laser Rabi frequency (circles). Vertical error bars from the fits. Horizontal errors: 10% uncertainty on the probe intensity. Dotted lines: results of the NCD model including the experimental parameters. Shaded area: uncertainty in the filling fraction $\eta = 0.5 \pm 0.1$. (b) Mean-field nonlinear coupled-dipole calculations for chains of N atoms (solid lines) are in reasonable agreement with a full quantum model (circles).

The reduction of the resonance shift can be interpreted as an effect of the saturation of individual quantum emitters [25]. Indeed, from the above nonlinear expression of the polarizability, the atomic dipole scales as $1/\Omega$ in the strong driving limit. Thus, on a given atom, the ratio of the driving applied by the other ones to the external driving decreases as $1/\Omega^2$, hence, suppressing interferences along the chain. The results of NCD calculations for the experimental parameters, involving ~100 atoms, are shown in Fig. 4(a). They are in good agreement with the experimentally measured global shift for the weakest driving, but predict a more gradual tailing off to zero for stronger driving. Further investigations are required to elucidate the disagreement at large driving amplitudes. A further reduction of interferences could also be due to incoherent scattered light, and in the strong field limit, some unaccounted-for mechanisms might pump atoms out of the two-level system.

The measurements presented here show that controlling the geometrical arrangement of an atomic sample allows us to shape its collective response to light, as also observed in [17]. Further investigations beyond the classical regime of

weak driving should follow. Increasing the coupling strength by reducing the interatomic distance will be a promising way forward for observing effects beyond what are captured by the mean-field model and to address long-lived subradiant states.

We would like to thank, D. Barredo, F. Nogrette, Y. Sortais, and W. Wu for assistance in early stages of the experiment, and T. Pohl, B. Olmos, J. Needham, J. Ruostekoski, D. Chang, R. Bettles, A. Asenjo-Garcia, and H. Ritsch for discussions. This work benefited from financial support by the Région Île-de-France in the framework of Domaine d'Intérêt Majeur (DIM) Nano-K (Project No. LISCOLEM) and DIM SIRTEQ (Project No. DSHAPE), and by "Investissements d'Avenir" LabEx PALM (Project No. ECONOMIQUE). N. Š. is supported by EU Horizon 2020 (COQUDDE, Marie Skłodowska-Curie Fellowship No. 786702). A. G. is supported by the Délégation Générale de l'Armement Fellowship No. 2018.60.0027.

*igor.ferrier-barbut@institutoptique.fr

[1] F. J. García De Abajo, Colloquium: Light scattering by particle and hole arrays, Rev. Mod. Phys. **79**, 1267 (2007).
[2] R. J. Bettles, S. A. Gardiner, and C. S. Adams, Enhanced Optical Cross Section Via Collective Coupling of Atomic Dipoles in a 2D Array, Phys. Rev. Lett. **116**, 103602 (2016).
[3] E. Shahmoon, D. S. Wild, M. D. Lukin, and S. F. Yelin, Cooperative Resonances in Light Scattering From Two-Dimensional Atomic Arrays, Phys. Rev. Lett. **118**, 113601 (2017).
[4] G. Scuri, Y. Zhou, A. A. High, D. S. Wild, C. Shu, K. De Greve, L. A. Jauregui, T. Taniguchi, K. Watanabe, P. Kim, M. D. Lukin, and H. Park, Large Excitonic Reflectivity of Monolayer $MoSe_2$ Encapsulated in Hexagonal Boron Nitride, Phys. Rev. Lett. **120**, 037402 (2018).
[5] P. Back, S. Zeytinoglu, A. Ijaz, M. Kroner, and A. Imamoglu, Realization of an Electrically Tunable Narrow-Bandwidth Atomically Thin Mirror Using Monolayer $MoSe_2$, Phys. Rev. Lett. **120**, 037401 (2018).
[6] H. Bender, C. Stehle, S. Slama, R. Kaiser, N. Piovella, C. Zimmermann, and P. W. Courteille, Observation of cooperative Mie scattering from an ultracold atomic cloud, Phys. Rev. A **82**, 011404(R) (2010).
[7] J. Pellegrino, R. Bourgain, S. Jennewein, Y. R. P. Sortais, A. Browaeys, S. D. Jenkins, and J. Ruostekoski, Observation of Suppression of Light Scattering Induced by Dipole-Dipole Interactions in a Cold-Atom Ensemble, Phys. Rev. Lett. **113**, 133602 (2014).
[8] W. Guerin, M. O. Araújo, and R. Kaiser, Subradiance in a Large Cloud of Cold Atoms, Phys. Rev. Lett. **116**, 083601 (2016).
[9] M. O. Araújo, I. Krešić, R. Kaiser, and W. Guerin, Superradiance in a Large and Dilute Cloud of Cold Atoms in the Linear-Optics Regime, Phys. Rev. Lett. **117**, 073002 (2016).
[10] S. J. Roof, K. J. Kemp, M. D. Havey, and I. M. Sokolov, Observation of Single-Photon Superradiance and the Cooperative Lamb Shift in an Extended Sample of Cold Atoms, Phys. Rev. Lett. **117**, 073003 (2016).
[11] S. Jennewein, M. Besbes, N. J. Schilder, S. D. Jenkins, C. Sauvan, J. Ruostekoski, J.-J. Greffet, Y. R. P. Sortais, and A. Browaeys, Coherent Scattering of Near-Resonant Light by a Dense Microscopic Cold Atomic Cloud, Phys. Rev. Lett. **116**, 233601 (2016).
[12] W. Guerin, M. T. Rouabah, and R. Kaiser, Light interacting with atomic ensembles: Collective, cooperative and mesoscopic effects, J. Mod. Opt. **64**, 895 (2017).
[13] S. L. Bromley, B. Zhu, M. Bishof, X. Zhang, T. Bothwell, J. Schachenmayer, T. L. Nicholson, R. Kaiser, S. F. Yelin, M. D. Lukin, A. M. Rey, and J. Ye, Collective atomic scattering and motional effects in a dense coherent medium, Nat. Commun. **7**, 11039 (2016).
[14] L. Corman, J. L. Ville, R. Saint-Jalm, M. Aidelsburger, T. Bienaimé, S. Nascimbène, J. Dalibard, and J. Beugnon, Transmission of near-resonant light through a dense slab of cold atoms, Phys. Rev. A **96**, 053629 (2017).
[15] S. Jennewein, L. Brossard, Y. R. P. Sortais, A. Browaeys, P. Cheinet, J. Robert, and P. Pillet, Coherent scattering of near-resonant light by a dense, microscopic cloud of cold two-level atoms: Experiment versus theory, Phys. Rev. A **97**, 053816 (2018).
[16] G. Facchinetti and J. Ruostekoski, Interaction of light with planar lattices of atoms: Reflection, transmission, and cooperative magnetometry, Phys. Rev. A **97**, 023833 (2018).
[17] J. Rui, D. Wei, A. Rubio-Abadal, S. Hollerith, J. Zeiher, D. M. Stamper-Kurn, C. Gross, and I. Bloch, A subradiant optical mirror formed by a single structured atomic layer, arXiv:2001.00795.
[18] D. Plankensteiner, L. Ostermann, H. Ritsch, and C. Genes, Selective protected state preparation of coupled dissipative quantum emitters, Sci. Rep. **5**, 16231 (2015).
[19] S.-T. Chui, S. Du, and G.-B. Jo, Subwavelength transportation of light with atomic resonances, Phys. Rev. A **92**, 053826 (2015).
[20] J. A Needham, I. Lesanovsky, and B. Olmos, Subradiance-protected excitation transport, New J. Phys. **21**, 073061 (2019).
[21] R. J. Bettles, S. A. Gardiner, and C. S. Adams, Cooperative eigenmodes and scattering in one-dimensional atomic arrays, Phys. Rev. A **94**, 043844 (2016).
[22] A. Asenjo-Garcia, M. Moreno-Cardoner, A. Albrecht, H. J. Kimble, and D. E. Chang, Exponential Improvement in Photon Storage Fidelities Using Subradiance and "Selective Radiance" in Atomic Arrays, Phys. Rev. X **7**, 031024 (2017).
[23] J. Javanainen, J. Ruostekoski, Y. Li, and S.-M. Yoo, Shifts of a Resonance Line in a Dense Atomic Sample, Phys. Rev. Lett. **112**, 113603 (2014).
[24] R. Jones, R. Saint, and B. Olmos, Far-field resonance fluorescence from a dipole-interacting laser-driven cold atomic gas, J. Phys. B **50**, 014004 (2017).
[25] L. A. Williamson and J. Ruostekoski, Optical response of atom chains beyond the limit of low light intensity: The validity of the linear classical oscillator model, Phys. Rev. Research **2**, 023273 (2020).
[26] S.-P. Yu, J. D. Hood, J. A. Muniz, M. J. Martin, R. Norte, C.-L. Hung, S. M. Meenehan, J. D. Cohen, O. Painter, and H. J. Kimble, Nanowire photonic crystal waveguides for

single-atom trapping and strong light-matter interactions, Appl. Phys. Lett. **104**, 111103 (2014).
[27] E. Vetsch, D. Reitz, G. Sagué, R. Schmidt, S. T. Dawkins, and A. Rauschenbeutel, Optical Interface Created by Laser-Cooled Atoms Trapped in the Evanescent Field Surrounding an Optical Nanofiber, Phys. Rev. Lett. **104**, 203603 (2010).
[28] P. Solano, P. Barberis-Blostein, F. K. Fatemi, L. A. Orozco, and S. L. Rolston, Super-radiance reveals infinite-range dipole interactions through a nanofiber, Nat. Commun. **8**, 1857 (2017).
[29] N. V. Corzo, J. Raskop, A. Chandra, A. S. Sheremet, B. Gouraud, and J. Laurat, Waveguide-coupled single collective excitation of atomic arrays, Nature (London) **566**, 359 (2019).
[30] A. S. Prasad, J. Hinney, S. Mahmoodian, K. Hammerer, S. Rind, P. Schneeweiss, A. S. Srensen, J. Volz, and A. Rauschenbeutel, Correlating photons using the collective nonlinear response of atoms weakly coupled to an optical mode, arXiv:1911.09701.
[31] Z. Meir, O. Schwartz, E. Shahmoon, D. Oron, and R. Ozeri, Cooperative Lamb Shift in a Mesoscopic Atomic Array, Phys. Rev. Lett. **113**, 193002 (2014).
[32] R. T. Sutherland and F. Robicheaux, Collective dipole-dipole interactions in an atomic array, Phys. Rev. A **94**, 013847 (2016).
[33] S. Krämer, L. Ostermann, and H. Ritsch, Optimized geometries for future generation optical lattice clocks, Europhys. Lett. **114**, 14003 (2016).
[34] T. S. do Espirito Santo, P. Weiss, A. Cipris, R. Kaiser, W. Guerin, R. Bachelard, and J. Schachenmayer, Collective excitation dynamics of a cold atom cloud, Phys. Rev. A **101**, 013617 (2020).
[35] J. Ruostekoski and J. Javanainen, Quantum field theory of cooperative atom response: Low light intensity, Phys. Rev. A **55**, 513 (1997).
[36] S. A. Aljunid, M. K. Tey, B. Chng, T. Liew, G. Maslennikov, V. Scarani, and C. Kurtsiefer, Phase Shift of a Weak Coherent Beam Induced by a Single Atom, Phys. Rev. Lett. **103**, 153601 (2009).
[37] M. Pototschnig, Y. Chassagneux, J. Hwang, G. Zumofen, A. Renn, and V. Sandoghdar, Controlling the Phase of a Light Beam with a Single Molecule, Phys. Rev. Lett. **107**, 063001 (2011).
[38] M. Celebrano, P. Kukura, A. Renn, and V. Sandoghdar, Single-molecule imaging by optical absorption, Nat. Photonics **5**, 95 (2011).
[39] E. W. Streed, A. Jechow, B. G. Norton, and D. Kielpinski, Absorption imaging of a single atom, Nat. Commun. **3**, 933 (2012).
[40] W. Alt, D. Schrader, S. Kuhr, M. Müller, V. Gomer, and D. Meschede, Single atoms in a standing-wave dipole trap, Phys. Rev. A **67**, 033403 (2003).
[41] N. Schlosser, G. Reymond, I. Protsenko, and P. Grangier, Sub-poissonian loading of single atoms in a microscopic dipole trap, Nature (London) **411**, 1024 (2001).
[42] N. Bruno, L. C. Bianchet, V. Prakash, N. Li, N. Alves, and M. W. Mitchell, Maltese cross coupling to individual cold atoms in free space, Opt. Express **27**, 31042 (2019).
[43] D. Rio Fernandes, F. Sievers, N. Kretzschmar, S. Wu, C. Salomon, and F. Chevy, Sub-Doppler laser cooling of fermionic ^{40}K atoms in three-dimensional gray optical molasses, Europhys. Lett. **100**, 63001 (2012).
[44] A. T. Grier, I. Ferrier-Barbut, B. S. Rem, M. Delehaye, L. Khaykovich, F. Chevy, and C. Salomon, Λ-enhanced sub-Doppler cooling of lithium atoms in D_1 gray molasses, Phys. Rev. A **87**, 063411 (2013).
[45] M. O. Brown, T. Thiele, C. Kiehl, T.-W. Hsu, and C. A. Regal, Gray-Molasses Optical-Tweezer Loading: Controlling Collisions for Scaling Atom-Array Assembly, Phys. Rev. X **9**, 011057 (2019).
[46] We have numerically checked that the shifts calculated by the steady-state model are the same as the one obtained by the time-dependent coupled-dipole model.
[47] See Supplemental Material at http://link.aps.org/supplemental/10.1103/PhysRevLett.124.253602 for details of the theoretical models and experimental protocols, which includes Refs. [48,49].
[48] M. Gross and S. Haroche, Superradiance: An essay on the theory of collective spontaneous emission, Phys. Rep. **93**, 301 (1982).
[49] R. H. Lehmberg, Radiation from an N-atom system. I. General formalism, Phys. Rev. A **2**, 883 (1970).
[50] In 1D, the field of the dipoles scattered along the chain is also σ_+ polarized, and therefore, one does not need to resort to the application of a large magnetic field to isolate a two-level structure, as was done for a random ensemble [15]. In this case, the Green's function $G(\boldsymbol{r})$ is also a scalar [47].
[51] R. Friedberg, S. R. Hartmann, and J. T. Manassah, Frequency shifts in emission and absorption by resonant systems of two-level atoms, Phys. Rep. **7**, 101 (1973).
[52] Note that, although it may look like this argument implies guiding of the light along the chain, guided modes exist only for a spacing smaller than $\lambda_0/2$, see Refs. [21,22].
[53] G. Grynberg, A. Aspect, and C. Fabre, *Introduction to Quantum Optics* (Cambridge University Press, Cambridge, 2010).
[54] S. Krämer and H. Ritsch, Generalized mean-field approach to simulate the dynamics of large open spin ensembles with long range interactions, Eur. Phys. J. D **69**, 282 (2015).
[55] C. D. Parmee and N. R. Cooper, Phases of driven two-level systems with nonlocal dissipation, Phys. Rev. A **97**, 053616 (2018).